Thermotropic biaxial nematic order parameters and phase transitions deduced by Raman scattering

2008 EPL 82 56001

(http://iopscience.iop.org/0295-5075/82/5/56001)

epl A Letters Journal Exploring the Frontiers of Physics

June 2008

EPL, **82** (2008) 56001 www.epljournal.org
doi: 10.1209/0295-5075/82/56001

Thermotropic biaxial nematic order parameters and phase transitions deduced by Raman scattering

C. D. Southern[1], P. D. Brimicombe[1], S. D. Siemianowski[1], S. Jaradat[1], N. Roberts[1], V. Görtz[2], J. W. Goodby[2] and H. F. Gleeson[1(a)]

[1] *School of Physics and Astronomy, The University of Manchester - Manchester, M13 9PL, UK, EU*
[2] *Department of Chemistry, The University of York, Heslington - York, YO10 5DD, UK, EU*

received 27 December 2007; accepted in final form 17 April 2008
published online 26 May 2008

PACS 61.30.-v – Liquid crystals
PACS 61.30.Gd – Orientational order of liquid crystals; electric and magnetic field effects on order
PACS 78.30.-j – Infrared and Raman spectra

Abstract – Raman Scattering was used to investigate biaxiality in the nematic phase formed by the bent-core material, C5-Ph-ODBP-Ph-OC12. Linearly polarised light was normally incident on a homogeneously aligned sample, and the depolarisation ratio was measured over a 360° rotation of the incident polarisation for the Raman-active phenyl stretching mode. By modeling the bent-core structure and fitting to the depolarisation data, both the uniaxial ($\langle P_{200}\rangle$ and $\langle P_{400}\rangle$) and biaxial ($\langle P_{220}\rangle$, $\langle P_{420}\rangle$ and $\langle P_{440}\rangle$) order parameters, are deduced. We show unequivocally the presence of a uniaxial to biaxial nematic phase transition approximately 30 °C above the underlying smectic phase. Further, we report the temperature evolution of the biaxial and uniaxial order parameters, which increase in magnitude continuously with reducing temperature, reaching values of 0.1, −0.15 and −0.18 for $\langle P_{220}\rangle$, $\langle P_{420}\rangle$ and $\langle P_{440}\rangle$, respectively.

Introduction. – In his 1970 paper [1], Freiser proposed the existence of a new nematic phase by considering a reduction in molecular symmetry. This reduced molecular symmetry would allow for the alignment of both the major and minor molecular axes, resulting in a biaxial nematic phase, fig. 1. The potential for a thermotropic biaxial nematic phase has been a topic of much debate in the liquid-crystal community since its discovery in lyotropic systems, formed from micellar aggregates [2]. The synthesis of many biaxial mesogens resulted, mainly formed from linked rod and disc structures, with the first report of a thermotropic biaxial nematic phase in 1986 [3]. However, for this and other materials the nematic biaxiality was not subsequently confirmed [4–6].

Since their inception bent-core liquid-crystalline materials have received a great deal of attention, due in part to the discovery of a completely new class of liquid-crystal phases, known as the B-phases [7]. This new set of B-phases result from the unique way in which the bent-core molecules can pack, owing to their intrinsic molecular biaxiality. However, if alignment of both the major and minor molecular axes can be achieved within a nematic phase, either through a true thermodynamic uniaxial to biaxial phase transition, or by means of coupling to an applied electric field, bent-core materials are strong contenders for the elusive biaxial nematic phase [8], fig. 1. Indeed, theoretical models of two linked rod-like units, based on attractive and repulsive molecular interactions, have successfully produced phase diagrams predicting the presence of the biaxial nematic phase [9,10]. The usefulness of these theoretical descriptions becomes apparent if one considers the bend angle which most stabilises the

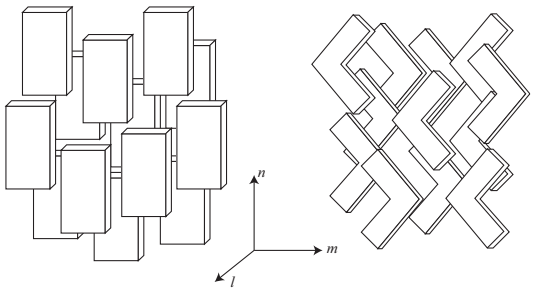

Fig. 1: Depiction of the biaxial nematic phase, formed by simple board-like and bent-core molecules. The biaxial nematic phase is defined by the alignment of the three molecular axes, n, m and l.

(a) E-mail: helen.gleeson@manchester.ac.uk

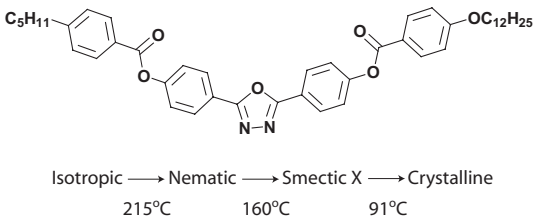

Fig. 2: The molecular schematic for the bent-core material C5-Ph-ODBP-Ph-OC12 and phase transitions observed in DSC cooling cycles at 10 °C per minute [18].

biaxial phase; indeed a bend angle approaching 110° is most conducive to forming the biaxial nematic phase.

Recently, a number of significant papers have been published showing biaxiality in the nematic phases formed by several bent-core materials (ODBP-Ph-C7, ODBP-Ph-OC12 and OxBP-Ph-OC12), measured using NMR spectroscopy and conoscopy [11] and X-ray diffraction [12,13]. Molecular modelling of these materials shows the bend angle to be approximately 140°, which is not consistent with the theoretical predictions. However, it appears that the large molecular dipole, neglected in the theory, that is present in these and other materials, seeks to stabilise the formation of the biaxial nematic phase for larger bend angles. Whilst X-ray diffraction was only able to indicate the presence of biaxiality, the NMR analysis was able to extract a quantitative biaxial parameter, η, equal to 0.1. Further discussion and comments have been published regarding the analysis in ref. [11], concerning the true nature of the measured biaxiality [14,15]. In addition, a number of other bent-core materials have been reported to exhibit biaxiality [16], and more recently, in a publication by Dong *et al.* [17], the biaxial order parameters were measured for the individual phenyl rings within a bent-core molecule using ^{13}C NMR spectroscopy.

In this letter we report the biaxial properties of the bent-core mesogen C5-Ph-ODBP-Ph-OC12, see fig. 2, which has been shown to exhibit unusual properties in the nematic phase via polarising microscopy [18]. In this investigation we employ both polarising Raman spectroscopy (PRS) and small-angle X-ray scattering (SAXS) as a means to elucidate the biaxial nature of the nematic phase formed by C5-Ph-ODBP-Ph-OC12. Whilst SAXS is a rather elegant technique for observing the director structure, and hence suggesting the presence of biaxiality, Raman scattering is one of the few techniques that can provide a means for quantifying biaxial ordering [19,20].

Polarised Raman scattering. – Polarised spectroscopy offers a robust technique for measuring the uniaxial and biaxial order parameters associated with liquid-crystal phases [21,22]. PRS probes the 2nd-rank tensorial differential polarisability, α'_{ji}, associated with vibrationally active modes. Using a single-excitation wavelength, these Raman active modes produce a spectral (or Raman) shift in the scattered radiation, allowing

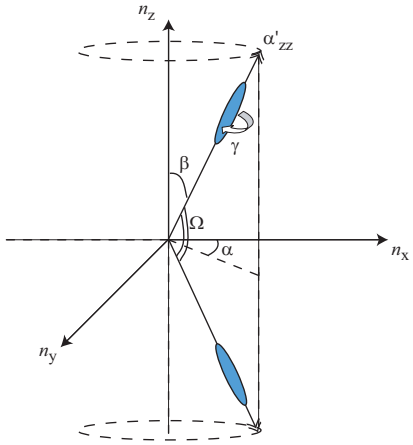

Fig. 3: The modelled bent-core molecule: containing two independent scatterers at an angular separation, Ω, of 140°.

one to isolate single modes by their characteristic shift in wavelength. The intensity of the scattered light is proportional to the square of the differential polarisability, providing information on both the 2nd- and 4th-rank ordering terms in the orientational distribution function (ODF),

$$I \propto \left(\frac{\partial \alpha'_{ji}}{\partial q_k} \right)^2 . \tag{1}$$

Indeed, PRS has been used successfully to determine the uniaxial order parameters, $\langle P_2 \rangle$ and $\langle P_4 \rangle$ (these are equivalent to $\langle P_{200} \rangle$ and $\langle P_{400} \rangle$), associated with standard nematic phases [23,24], by using a judicious choice of sample geometry. Further it was shown that by measuring the intensity from an active mode through a 360° rotation of the incident polarisation vector, one can obtain much more reliable order parameter data [25,26], together with the possible inclusion of biaxial ordering terms [19,20]. It is worth noting that the subsequent notation used to express the order parameters will retain the subscripts expressing the phase and molecular-symmetry assumptions, $\langle P_{L,m,n} \rangle$.

Using a Renishaw Raman spectrometer, operating at 514 nm and at a power of 10 mW, and coupled to a Leica DML polarising microscope, the full Raman spectrum was measured in the nematic phase of C5-Ph-ODBP-Ph-OC12. In order to detect the presence of phase biaxiality, it is imperative that a suitable probe is used. The strongest Raman active mode is, as expected, the phenyl stretching mode observed at 1606 cm^{-1}; this is also the most widely used and characterised probe band [24–26]. The reported uniaxiality of the phenyl stretching mode [24–26] requires that the molecular biaxiality be reflected by the position and orientation of the phenyl rings on the molecule. Fortuitously, C5-Ph-ODBP-Ph-OC12 contains a symmetric distribution of phenyl rings on each of the molecular arms, with an approximate 140° [11,13,27] offset in the major vibration axis, see fig. 3.

An additional advantage of such a system, is that, since the vibrational probe is itself uniaxial, it is the bend

$$f(\alpha,\beta) = \frac{1}{8\pi^2}\Bigg[1 + \frac{5}{2}\langle P_{200}\rangle(3\cos^2(\beta)-1) + \frac{5}{2}\langle P_{220}\rangle 6(1-\cos^2(\beta))\cos(2\alpha) + \frac{9}{8}\langle P_{400}\rangle(3-30\cos^2(\beta)+35\cos^4(\beta)) + \frac{9}{8}\langle P_{420}\rangle 60(-1+8\cos^2(\beta)-7\cos^4(\beta))\cos(2\alpha) + \frac{9}{8}\langle P_{440}\rangle 70(1-2\cos^2(\beta)+\cos^4(\beta))\cos(4\alpha)\Bigg]. \quad (5)$$

angle that defines the molecular biaxiality, thereby eliminating the molecular-biaxiality terms when one comes to define the ODF.

Cooling from the isotropic phase of the sample was held, and intensity measurements taken at the following reduced temperatures ($T - T_{\rm NI}$): $-3\,^\circ$C, $-8\,^\circ$C, $-18\,^\circ$C, $-28\,^\circ$C, $-38\,^\circ$C, $-48\,^\circ$C and $-58\,^\circ$C, where the isotropic to nematic transition temperature is defined as zero and the lowest-temperature measurement was just before the transition to the underlying smectic X phase. At each temperature the scattered intensity from the phenyl stretching mode was measured over a 360° rotation of the incident polarisation for two analyser orientations, firstly, the analyser parallel to the incident polarisation, and secondly, with the analyser perpendicular to the incident polarisation.

The expressions governing the observed intensities are as follows:

$$I_{\parallel}(\theta) = I_0 \int_\alpha \int_\beta \int_\gamma f(\alpha,\beta,\gamma)\big(E_{\parallel}(\alpha,\beta,\gamma)\big)^2 {\rm d}\alpha{\rm d}\beta{\rm d}\gamma, \quad (2)$$

$$I_{\perp}(\theta) = I_0 \int_\alpha \int_\beta \int_\gamma f(\alpha,\beta,\gamma)(E_{\perp}(\alpha,\beta,\gamma))^2 {\rm d}\alpha{\rm d}\beta{\rm d}\gamma, \quad (3)$$

where I_0 is the incident intensity, and $E(\alpha,\beta,\gamma)$ is the scattered electric-field vector.

More importantly, the ODF, $f(\alpha,\beta,\gamma)$, requires sufficient definition. The ODF describes the statistically averaged orientation of the axes of symmetry of a system and is defined by the summation of the set of Wigner functions, $D^L_{mn}(\alpha,\beta,\gamma)$:

$$f(\alpha,\beta,\gamma) = \sum_{L=0}^{\infty}\sum_{m=-L}^{+L}\sum_{n=-L}^{+L}\frac{2L+1}{8\pi^2}\langle D^{L^*}_{mn}\rangle D^L_{mn}(\alpha,\beta,\gamma). \quad (4)$$

A discussion of the symmetry relations is reported in detail by van Gurp [28], and with respect to liquid-crystal phases specifically by Zannoni [29]. These can be summarised as follows for a standard non-polar and non-chiral nematic system: due to the symmetry of the system we are unable to distinguish between any 180° rotation, and as a result L, m and n must take even values. Due to the uniaxial nature of the probe Raman mode the molecular biaxiality is defined by the molecular-bend angle, and as a consequence, the terms defining the molecular biaxiality, $n \neq 0$, are zero. Allowing for these assumptions and expanding the ODF to include the presence of phase biaxiality only, the ODF can be expressed as [20]

see eq. (5) *above*

In eq. (5) the order parameters are defined by the generalised Legendre polynomials, $\langle P_{L,m,n}\rangle$. The definition of the ODF allows the observed intensity profiles for each of the analyser orientations to be modelled, and the order parameters determined [25,26]. In order to eliminate the incident intensity, I_0, from eqs. (2) and (3) one can define the depolarisation ratio, R:

$$R(\theta) = \frac{I_{\perp}(\theta)}{I_{\parallel}(\theta)}. \quad (6)$$

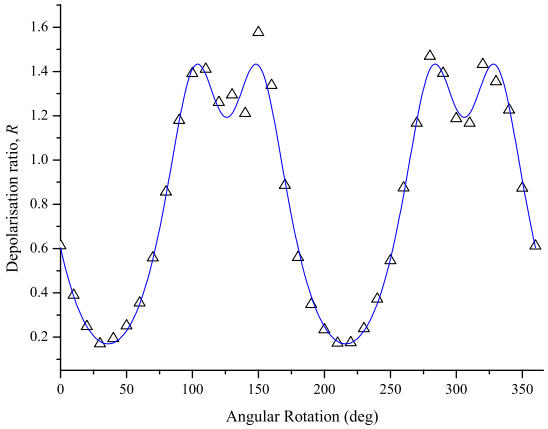

Fig. 4: The experimental depolarisation ratio, R [△], together with the modelled bent-core profile for C5-Ph-ODBP-Ph-OC12 held at $T - T_{\rm NI} = -18\,^\circ$C.

Figure 4 shows $R(\theta)$ measured for C5-Ph-ODBP-Ph-OC12 held at a reduced temperature, $T - T_{\rm NI} = -18\,^\circ$C. By modeling the bent-core system, using eqs. (2), (3) and (6), a χ^2 minimisation routine was employed to determine the best-fit order parameters, $\langle P_{L,m,0}\rangle$, for each of the measured depolarisation ratios. A bend angle of 140° [11,13,27] was used in the modelled system, and each of the molecular arms was considered as an independent scatterer. Figure 5 shows the best-fit biaxial order parameters, $\langle P_{220}\rangle$, $\langle P_{420}\rangle$ and $\langle P_{440}\rangle$, determined from the depolarisation ratio as a function of temperature.

The measured parameters show a clear uniaxial to biaxial transition at around $T - T_{\rm NI} = -28\,^\circ$C. Interestingly,

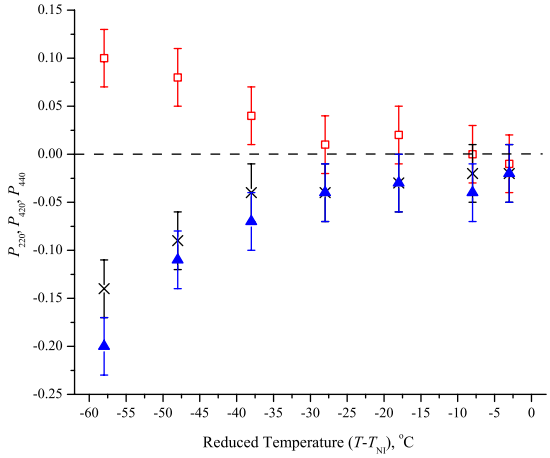

Fig. 5: The measured biaxial order parameters, $\langle P_{220}\rangle$ [□], $\langle P_{420}\rangle$ [×] and $\langle P_{440}\rangle$ [▲], obtained by fitting the depolarisation ratio profile, $R(\theta)$.

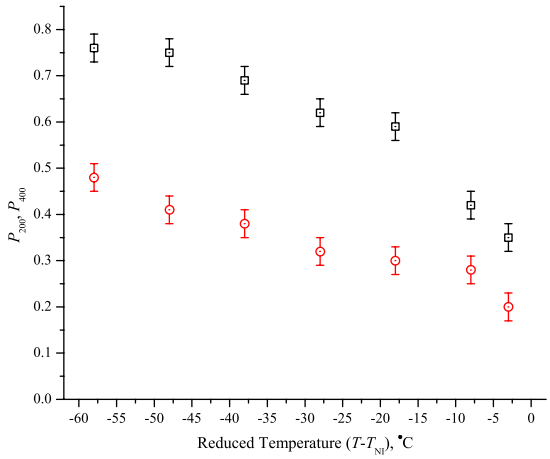

Fig. 6: The measured uniaxial order parameters, $\langle P_{200}\rangle$ [⊡] and $\langle P_{400}\rangle$ [⊙], obtained by fitting the depolarisation ratio profile.

the 4th-rank ordering terms, $\langle P_{420}\rangle$ and $\langle P_{440}\rangle$, appear to be negative; whilst, the 2nd-rank term, $\langle P_{220}\rangle$, takes positive values. In each case there is a clear trend, increasing the magnitude of the biaxial order parameters as the temperature is decreased. Our work can be compared to the negative biaxial values obtained by Dong *et al.* [17] for all but one of the phenyl rings present on a similar bent-core molecule, ranging between 0 and −0.2, in which the lowest values correspond to the centrally positioned phenyl ring, together with a single phenyl ring exhibiting positive values between 0.05 and 0.2. The magnitude and sign of these biaxial parameters are similar to the measured biaxiality presented here for the phase biaxiality as a whole, further supporting our conclusions. In addition, the forms of the measured uniaxial ordering parameters, $\langle P_{200}\rangle$ and $\langle P_{400}\rangle$, are also important, and are shown as a function of temperature in fig. 6. The best-fit uniaxial order parameters exhibit the expected magnitude and temperature dependence for such a wide nematic phase.

In order to validate the measured order parameters in figs. 5 and 6, it was important to ensure that inclusion of the biaxial terms in the ODF did not simply allow for an easier fit to the data. Thus, fits were also performed assuming a uniaxial model, which resulted in essentially identical uniaxial order parameters. Inclusion of the biaxial terms simply improved the fits. The fact that these biaxial terms return negligible values in the high-temperature nematic range ($T - T_{\mathrm{NI}} = 0$ to $-30\,^{\circ}\mathrm{C}$), further validates this approach.

We also note that the assumption that the bend angle is 140° in our model could lead to errors in the calculation of the magnitude of the order parameters, since the bend angle defines the molecular biaxiality. Specifically, the order parameters are defined by the molecular fluctuations allowed by the phase, and as such, an error in the static bend angle would not impinge on the measured temperature trends, only the magnitude of the parameters. In order to quantify this dependence, the fitting procedure was employed assuming a ±5° error in the bend angle. Applying the upper and lower limits shows an additional uncertainty introduced to $\langle P_{220}\rangle$, $\langle P_{420}\rangle$ and $\langle P_{440}\rangle$ of ±0.02. It was also found that the uniaxial parameters, $\langle P_{200}\rangle$ and $\langle P_{400}\rangle$, and r are insensitive to such small changes in the assumed bend angle.

Small-angle X-ray scattering (SAXS). – The X-ray scattering from a uniaxial nematic phase formed by a liquid crystal is known to produce two sets of diffuse peaks. The first result from the end-to-end correlation of the molecules and equate, approximately, to the molecular length, typically observed in the small angle. The second are produced by the side-to-side correlation of the molecules, and due to the relatively short length scales, are observed in the wide-angle geometry.

In the case of bent-core molecules the situation is more complicated, though X-ray diffraction can provide a rather elegant method for visualising the director correlation of the two molecular arms. In a system of bent-core molecules there exists two contributions to the scattering, as a result of the concentration in the electron density along each of the molecular arms. It has been suggested that in a biaxially aligned system, the molecular bend can be resolved by a splitting of the uniaxial diffraction peaks into a four-peak diffraction pattern [12,13]. Significant care must be taken, however, in interpreting the resultant diffraction, since a four-peak structure is not on its own a definitive indicator of biaxiality. Indeed, questions have been raised regarding the validity of this approach [30]. The following X-ray diffraction results are therefore presented as supplementary to the biaxial order parameters obtained from PRS.

The SAXS experiments were performed on station 2.1 at the Synchrotron Radiation Source, Daresbury Laboratory, UK, operating at a wavelength of 1.54 Å. The material was sandwiched between two mica windows, and crimped together using a modified DSC pan. The mica windows

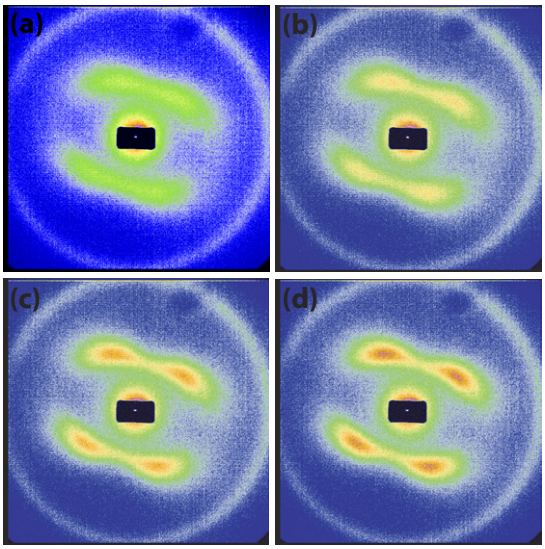

Fig. 7: The SAXS patterns from the nematic phase of C5-Ph-ODBP-Ph-OC12. Each image represents the accumulative scattering from a 3-minute exposure, at a cooling rate of 0.5 degrees per minute. Calibrating each of the images to a reduced temperature gives: (a) frame 15 (−15 °C); (b) frame 25 (−30 °C); (c) frame 35 (−45 °C); and (d) frame 40 (−53 °C). The outer diffraction ring shown is due to the Kapton windows used to insulate the temperature oven.

were used to align the nematic phase; no electric or magnetic fields were applied. The sample temperature was controlled using a Linkam hot-stage and temperature controller, mounted vertically onto the beamline. The diffracted X-rays are incident on a two-dimensional area detector, positioned 1 m from the sample. Figure 7 shows the sequence of diffraction images obtained throughout the nematic phase on continuous cooling from the isotropic phase. As before, the temperatures are presented on a reduced scale from the isotropic to nematic transition. Each image represents the accumulated scattering from a 3-minute exposure, at a continuous cooling rate of 0.5 °C per minute. One will notice that fig. 7 shows a slowly evolving four-peak scattering pattern. Although there is a hint of a four-peak structure at high temperatures, one can clearly resolve four distinct peaks only below a reduced temperature of around −30 °C, with an increased intensity observed at each of the four diffraction positions on further cooling.

Performing further analysis on the observed diffraction images allows the calculation of both the angular peak separation, ρ, and the spatial peak position, l, see insets in figs. 8 and 9. Figure 8 shows the angular peak separation, defined in the inset, which is seen to saturate at 76° and 104°. Using silver behenate as a calibration, with known crystalline structure, one can measure the spatial peak position, l, from the observed diffraction and make a direct calculation regarding the end-to-end length correlations of the molecules. Figure 9 shows that the length correlations exhibit no temperature dependence, with a

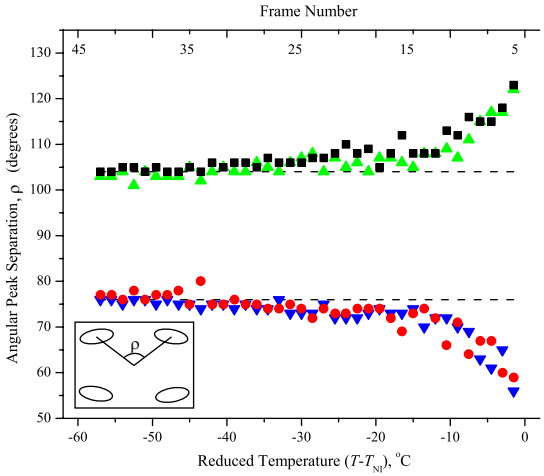

Fig. 8: The angular separation of the four observed diffraction peaks (each represented by a different symbol) as a function of temperature. Due to the symmetry of the phase we observe a saturation in the angular peak separation of 76° and 104°.

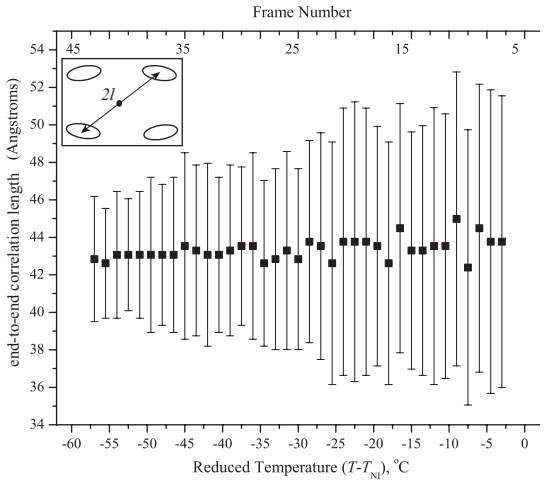

Fig. 9: The end-to-end correlation length as a function of temperature. An average spacing of 43 Å corresponds approximately to the molecular length and shows no temperature dependence.

calculated spacing of 43 Å corresponding approximately to the molecular length.

Following the interpretation of Acharya [12,13], the angular peak separation, together with the intensity evolution of the observed peaks, could suggest that, rather than a random distribution of the molecular arms around the long axis of the molecules, there exist domains in which an increasing proportion of molecules are ordered with their molecular arms in the diffraction plane. The observed X-ray scattering intensity, $I(q)$, can be expressed as the product of the form factor (a Fourier transform of the molecular electron density), $f(q)$, and the structure factor (describing the inter-molecular electron density correlations), $S(q)$:

$$I(q) = f(q) \times S(q), \tag{7}$$

where q is the reciprocal space co-ordinate.

In simulations using the form factor for a bent-core molecule, with a modelled molecular bend of 140°, splitting in the small-angle scattering peaks was observed [13]. It is worth noting that, although the oxadiazole core is relatively rigid, the terminal groups can undergo a variety of conformational changes, making the modelled bend angle somewhat arbitrary. Interestingly, the observed peak spacings of 80° and 100°, for a perfectly biaxially aligned nematic phase, correspond very closely with our experimentally observed four-peak diffraction pattern. These diffraction data are not, however, a definitive indicator of biaxiality and pre-transitional smectic (cybotactic) grouping is a possibility that must be considered. In support of the biaxial interpretation, the end-to-end length correlations correspond, approximately, to the molecular length and show no temperature dependence. Indeed SAX measurements on the underlying smectic phase show a temperature-dependent layer spacing and no bulk alignment. In addition, the angular peak separation of 76° matches almost precisely to the simulated biaxial diffraction pattern, with a predicted angular peak separation of 80° [13], corresponding to the expected molecular-bend angle of approximately 140° [11,13,27]. However, to truly rule out the possibility of cybotactic groups contributing to the observed diffraction, further experiment and clarification are required. Thus, we note that our X-ray diffraction results offer consistency with the biaxial order parameters measured via PRS, rather than providing an independent measurement of biaxiality.

Conclusions. – We have produced polarised Raman scattering data that confirm the existence of a thermotropic biaxial nematic phase in C5-Ph-ODBP-Ph-OC12 in the absence of any external magnetic or electric fields, supported by X-ray scattering. The temperature-dependent Raman scattering depolarisation ratio has been analysed in the context of both uniaxial and biaxial assumptions, leading to the determination of non-zero biaxial order parameters in the lower-temperature regime of the nematic phase of C5-Ph-ODBP-Ph-OC12. We therefore conclude that this interesting material exhibits a uniaxial to biaxial phase transition approximately 30° below the isotropic to nematic phase transition. We demonstrate that the uniaxial order parameters of both of the nematic phases increase continuously as temperature reduces. The biaxial order parameters are, unsurprisingly, negligible in the uniaxial phase, and increase in magnitude continuously as we probe deeper into the biaxial nematic phase range. This not only confirms nematic biaxiality in C5-Ph-ODBP-Ph-OC12, but also quantifies it.

* * *

The authors wish to thank EPSRC for their financial support and the SRS for supporting our beamtime application.

REFERENCES

[1] Freiser M. J., *Phys. Rev. Lett.*, **24** (1970) 1041.
[2] Yu L. J. and Saupe A., *Phys. Rev. Lett.*, **45** (1980) 1000.
[3] Malthête J., Nguyen H. T. and Levelut A. M., *J. Chem. Soc. Chem. Commun.*, issue No. 20 (1986) 1548.
[4] Fan S. M. *et al.*, *Chem. Phys. Lett.*, **204** (1993) 517.
[5] Shenouda I. G. Shi Y., Shi Y. and Neubert M. E., *Mol. Cryst. Liq. Cryst.*, **257** (1994) 209.
[6] Hughes J. R. *et al.*, *J. Chem. Phys.*, **107** (1997) 9252.
[7] Takezoe H. and Takanishi Y., *Jpn. J. Appl. Phys.*, **45** (2006) 597.
[8] Luckhurst G. R., *Angew. Chem. Int. Ed.*, **44** (2005) 2834.
[9] Teixeira P. I. C., Masters A. J. and Mulder B. M., *Mol. Cryst. Liq. Cryst.*, **323** (1998) 167.
[10] Luckhurst G. R., *Thin Solid Films*, **393** (2001) 40.
[11] Madsen L. A. *et al.*, *Phys. Rev. Lett.*, **92** (2004) 145505.
[12] Acharya B. R. *et al.*, *Pramana*, **61** (2003) 231.
[13] Acharya B. R., Primak A. and Kumar S., *Phys. Rev. Lett.*, **92** (2004) 145505.
[14] Galerne Y., *Phys. Rev. Lett.*, **96** (2006) 219803.
[15] Madsen L. A. *et al.*, *Phys. Rev. Lett.*, **96** (2006) 219804.
[16] Prasad V. *et al.*, *J. Am. Chem. Soc.*, **127** (2005) 17224.
[17] Dong R. Y., Kumar S., Prasad V. and Zhang J., *Chem. Phys. Lett.*, **448** (2007) 54.
[18] Görtz V. and Goodby J. W., *Chem. Commun.*, issue No. 26 (2005) 3262.
[19] Southern C. D. and Gleeson H. F., *Eur. Phys. J. E*, **24** (2007) 119.
[20] Jarvis D. A. *et al.*, *Polymer*, **21** (1980) 41.
[21] Ossowska-Chruściel M. D. *et al.*, *Phys. Rev. E*, **70** (2004) 041705.
[22] Merkel K. *et al.*, *Phys. Rev. Lett.*, **93** (2004) 237801.
[23] Jen S., Clark N. A., Pershan P. S. and Priestley E. B., *Phys. Rev. Lett.*, **31** (1973) 1552.
[24] Jen S., Clark N. A., Pershan P. S. and Priestley E. B., *J. Chem. Phys.*, **66** (1977) 4635.
[25] Jones W. J. *et al.*, *J. Mol. Struct.*, **614** (2002) 75.
[26] Jones W. J. *et al.*, *J. Mol. Struct.*, **708** (2004) 145.
[27] Dingemans T. J. and Samulski E. T., *Liq. Cryst.*, **27** (2000) 1316.
[28] van Gurp M., *Colloid Polym. Sci.*, **273** (1995) 607.
[29] Zannoni C., *The Molecular Physics of Liquid Crystals*, edited by Luckhurst G. R. and Gray G. W. (Academic Press) 1979, p. 51.
[30] Lee J. H. *et al.*, *J. Appl. Phys.*, **101** (2007) 034105.